

Azimuthal decorrelation for photon induced dijet production in ultra-peripheral collisions of heavy ions

Cheng Zhang^a, Qian-Shun Dai^a and Ding Yu Shao^{a,b}

^a*Department of Physics and Center for Field Theory and Particle Physics, Fudan University, Shanghai, China*

^b*Key Laboratory of Nuclear Physics and Ion-beam Application (MOE), Fudan University, Shanghai, China*

E-mail: chengzhang_phy@fudan.edu.cn, qs dai21@m.fudan.edu.cn,
dingyu.shao@cern.ch

ABSTRACT: We study the azimuthal angular decorrelation of the dijet production via photon fusion in ultra-peripheral heavy ion collisions. The impact parameter dependent cross section of quark-antiquark pairs production is derived using the equivalent photon approximation, and the contribution from final-state QCD radiations to the azimuthal angular distribution are calculated within Soft-Collinear Effective Theory. We carry out the QCD resummation of large logarithms of the azimuthal angle as well as the jet radius at next-to-leading logarithmic accuracy. In the end we present the normalized differential cross section for azimuthal decorrelation of the dijet pair and find that our results are consistent with the measurements reported by the ATLAS collaboration.

Contents

1	Introduction	1
2	Quark-antiquark pairs production from $\gamma\gamma$ fusions	3
3	Factorization and resummation for final-state radiations	5
3.1	QCD factorization formalism in SCET	6
3.2	QCD resummation formalism of final-state radiation	8
4	Numerical results	10
5	Conclusion	13
A	Soft, collinear-soft functions and the collinear anomaly	13
B	Anomalous dimension	14

1 Introduction

Ultrapерipheral collisions (UPCs) of high-energy nuclei are processes that the impact parameter is large enough so that only electromagnetic interactions happen with hadronic interactions being excluded. UPCs involve two-photon fusions and photonuclear interactions, which provide an opportunity to study the quasi-real photons emitted by one of the colliding nuclei and probe the nuclear parton distribution functions (PDFs). Typical photonuclear processes [1–10] involve the photoproduction of vector mesons via photon-gluon fusions, which is a clean probe to study the gluon distributions inside the energetic nucleus [11–21]. Typical two-photon interactions involve dilepton productions [22–28] or diphoton productions from light-by-light scatterings [29]. The dilepton production process can serve to probe the strong electromagnetic fields generated from the initial state relativistic heavy-ion [30–36], as well as the polarizations of the these quasi-real photons [37–39], or to study the final-state Quantum Electrodynamics (QED) radiations from the produced charged leptons.

The photon flux coherently emitted from the charged nucleus is highly enhanced by a factor of the squared nuclear charge Z^2 , and these photons are nearly real with a small virtuality $k^2 \lesssim (\hbar/R_A)^2$, where R_A is the nuclear radius. The quasi-real photon flux can be well described by the well known equivalent photon approximation (EPA) introduced by Fermi, von Weizsäcker and Williams [40–42], where the strong photon flux is treated as a highly Lorentz-contracted classical electromagnetic field emitted from the fast moving nucleus. Within the EPA method the photon spectrum is the Fourier transform of the nuclear charge spatial distribution.

Recently, in ultraperipheral $Pb + Pb$ collisions Quantum Chromodynamics (QCD) jets production in $0n0n$ events was first observed by the ATLAS collaboration [22], and they find PYTHIA8 Monte Carlo event generator [43] underestimates the total cross section by about an order of magnitude. Usually, dijet and multi-jet production in UPCs with no nuclear breakup involves both photon fusion and diffractive photo-production processes. This discrepancy in magnitude may result from the missing processes of the diffractive photo-production in PYTHIA8, and these processes has been calculated in [44], where the results are obtained by using the next-to-leading order (NLO) collinear factorization formalism of perturbative QCD (pQCD). Besides, in [22] the ATLAS collaboration also present the experimental results of the azimuthal angle $\Delta\phi_{jj}$ between the two jets with the highest transverse momenta. In order to directly compare the shape of the measured distribution with the PYTHIA results, they have rescaled the PYTHIA curve to match the number of measured events. As a result, they find the measured distribution is obviously wider than that from the PYTHIA8 event generator. Therefore, it is significant to have a theoretical calculation for the $\Delta\phi_{jj}$ -distribution.

Starting with the pioneering papers [45, 46], all-order resummation of azimuthal decorrelation for QCD jets has been performed in various processes [47–59]. Usually, fixed-order calculations in pQCD can be used to systematically improve the description of hadronic radiation. However, in nearly back-to-back region $\Delta\phi_{jj} \sim \pi$ the fixed-order expansion of pQCD diverges due to the existence of logarithms $\alpha_s^n \ln^m(\pi - \Delta\phi_{jj})$ (with $0 < m \leq 2n$) at each perturbative order n , so that an all-order resummation is necessary for the validity of theoretical predictions. Besides, as pointed in [45, 56] the all-order resummation formula strongly depends on the recombination schemes in sequential jet clustering algorithms. Especially when the jets are reconstructed with the p_T^n -weighted recombination scheme, the resummation is straightforward since it does not require any non-trivial treatment of non-global logarithms (NGLs) [60, 61].

In this paper we perform a detailed theoretical study for the azimuthal decorrelation of dijet productions from photon-photon fusion in ultraperipheral heavy ion collisions. Specifically, we consider the $\Delta\phi_{jj}$ -distribution of the leading dijet pair produced nearly back to back in the transverse plane to the beam. In order to describe such configuration we need to consider nonzero transverse momenta from both incoming and outgoing partons. First of all, since the initial photons can have nonzero transverse momentum, one needs to consider the transverse momentum dependent photon distribution. This effect can be captured by the impact parameter dependent cross section in EPA, and the corresponding calculations have been extensively studied in [19, 30, 32, 33, 35–39]. Moreover, final-state radiations could also introduce azimuthal angular decorrelation. We apply Soft-Collinear Effective Theory (SCET) [62–66] to develop a factorization and resummation formalism for studying the azimuthal angular distribution in back-to-back dijet production in ultraperipheral heavy ion collisions, where large logarithms of the azimuthal angle and the jet radius are resummed at next-to-leading logarithmic (NLL) accuracy.

The rest of this paper is organized as follows. In section 2 we discuss the impact parameter dependent cross section of quark-antiquark pairs production via photon-photon fusions in UPCs. In section 3 we give the factorization and resummation formula of $\gamma\gamma \rightarrow 2$ jets

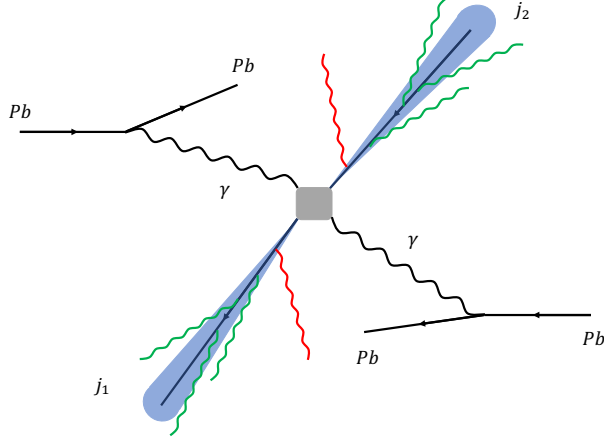


Figure 1. Photon-induced dijet production in UPCs.

within SCET. We present the numerical results using the theoretical formula, enumerate all theoretical uncertainties and compare our predictions with the ATLAS experimental data in section 4. We conclude in section 5. The details of the one-loop calculations, resummation, and anomalous dimensions are provided in the appendix.

2 Quark-antiquark pairs production from $\gamma\gamma$ fusions

In this section, we give the impact parameter dependent cross section of quark-antiquark pairs production from photon-photon fusions in UPCs at the lowest QED order, which provides the initial state of the dijet production. Associating that with the final-state QCD emissions, we arrive at the dijet production from two-photon interactions in UPCs. The two-photon fusion process reads,

$$\gamma(\omega_1, \mathbf{k}_{1T}) + \gamma(\omega_2, \mathbf{k}_{2T}) \rightarrow q(y_1, \mathbf{p}_{1T}) + \bar{q}(y_2, \mathbf{p}_{2T}). \quad (2.1)$$

After applying the Weizsäcker-Williams equivalent photon approximation (EPA) [40–42], one can drive the unpolarized UPC differential cross section as [32, 37, 38]

$$\begin{aligned} \frac{d^5\sigma_0}{d^2\mathbf{q}_T d p_T dy_1 dy_2} &= N_c \sum_q e_q^4 \frac{Z^4 \alpha_{\text{em}}^4}{\pi^5 M^4} p_T \int d^2\mathbf{b}_T d^2\mathbf{k}_{1T} d^2\mathbf{k}_{2T} d^2\mathbf{k}'_{1T} d^2\mathbf{k}'_{2T} \\ &\times \delta^{(2)}(\mathbf{k}_{1T} + \mathbf{k}_{2T} - \mathbf{q}_T) \delta^{(2)}(\mathbf{k}'_{1T} + \mathbf{k}'_{2T} - \mathbf{q}_T) e^{i(\mathbf{k}_{1T} - \mathbf{k}'_{1T}) \cdot \mathbf{b}_T} \\ &\times k_{1T} \frac{F(-k_1^2)}{-k_1^2} k_{2T} \frac{F(-k_2^2)}{-k_2^2} k'_{1T} \frac{F(-k_1'^2)}{-k_1'^2} k'_{2T} \frac{F(-k_2'^2)}{-k_2'^2} \frac{M^2 - 2p_T^2}{p_T^2} \\ &\times \cos\left(\phi_{\mathbf{k}_{1T}} - \phi_{\mathbf{k}'_{1T}} + \phi_{\mathbf{k}_{2T}} - \phi_{\mathbf{k}'_{2T}}\right), \end{aligned} \quad (2.2)$$

with the nuclear electric charge Z (79 for Au , 82 for Pb), the fine-structure constant $\alpha_{\text{em}} = 1/137$, the number of colors $N_c = 3$, the quark fractional electric charge e_q , and the quark flavors q . Since we only consider QCD light flavor jet production, the cross section is a sum over the light quark flavors $q = u, d, s$. Here we define the average transverse momentum \mathbf{p}_T of the two jets and the transverse momentum imbalance \mathbf{q}_T as follows

$$\mathbf{p}_T \equiv (\mathbf{p}_{1T} - \mathbf{p}_{2T})/2, \quad \mathbf{q}_T \equiv \mathbf{p}_{1T} + \mathbf{p}_{2T}. \quad (2.3)$$

The quark-antiquark pairs are produced nearly back-to-back in the transverse plane with respect to the beam direction, so the transverse momentum imbalance $q_T \equiv |\mathbf{q}_T|$ is small. In the limit of $q_T \ll p_T \sim p_{1T} \sim p_{2T}$, the invariant mass of quark-antiquark pairs reads

$$M = p_T \sqrt{2 + 2 \cosh(y_1 - y_2)}, \quad (2.4)$$

with quark rapidities $y_{1,2}$. The impact parameter b_T should be integrated over from $2R_A$ to ∞ to exclude the central collisions, where R_A is the nuclear radius. The photon possesses different transverse momentum \mathbf{k}_T (with the azimuthal angle $\phi_{\mathbf{k}_T}$) and \mathbf{k}'_T inside the amplitude and the conjugate amplitude respectively, as we have kept the impact parameter dependence of two colliding photon fluxes. The quasi-real photon flux with a small virtuality $k^2 = -\omega^2/\gamma^2 - \mathbf{k}_T^2$ (with the Lorentz boost factor $\gamma = 2676$ at a centre-of-mass energy per nucleon pair of $\sqrt{s_{\text{NN}}} = 5.02$ TeV at the CERN LHC) and photon energy $\omega_{1,2} = p_T(e^{\pm y_1} + e^{\pm y_2})/2$ can be described by the EPA, which depicts the photon momentum k distribution via the nuclear charge form factor $F(-k^2)$. This form factor can be obtained after performing Fourier transformation from the nuclear charge distribution $\rho(r)$ as

$$F(\mathbf{k}^2) = \int d^3\mathbf{r} e^{i\mathbf{r} \cdot \mathbf{k}} \rho(r), \quad (2.5)$$

where the charge distribution inside the heavy nucleus is well described by the Woods-Saxon distribution,

$$\rho_{\text{WS}}(r) = \frac{1}{1 + e^{(r-R_A)/d}} \bigg/ \int d^3\mathbf{r} \frac{1}{1 + e^{(r-R_A)/d}}, \quad (2.6)$$

with the nuclear radius $R_A \simeq 1.2 A^{1/3}$ (where A is the nucleon number) and the nuclear skin depth d ($d = 0.546$ fm for Pb and $d = 0.535$ fm for Au). In the left panel of figure 2 we plot the nuclear charge spatial distribution of lead (red solid curve) and gold (blue dashed curve) nuclei within the Woods-Saxon model. One can see that the lead nuclei possesses a slightly wider spatial broadening and a less steep boundary compared to the gold nuclei. For simplicity, in the latter calculation, we alternatively choose the approximate Woods-Saxon form factor used in the STARlight Monte Carlo event generator [67],

$$F_{\text{AWS}}(\kappa^2) = \frac{3[\sin(\kappa R_A) - \kappa R_A \cos(\kappa R_A)]}{(\kappa R_A)^3(a^2\kappa^2 + 1)}, \quad (2.7)$$

with $a = 0.7$ fm. The corresponding nuclear charge form factors are shown in the right panel of figure 2, and we find the difference between these two models is negligible. From

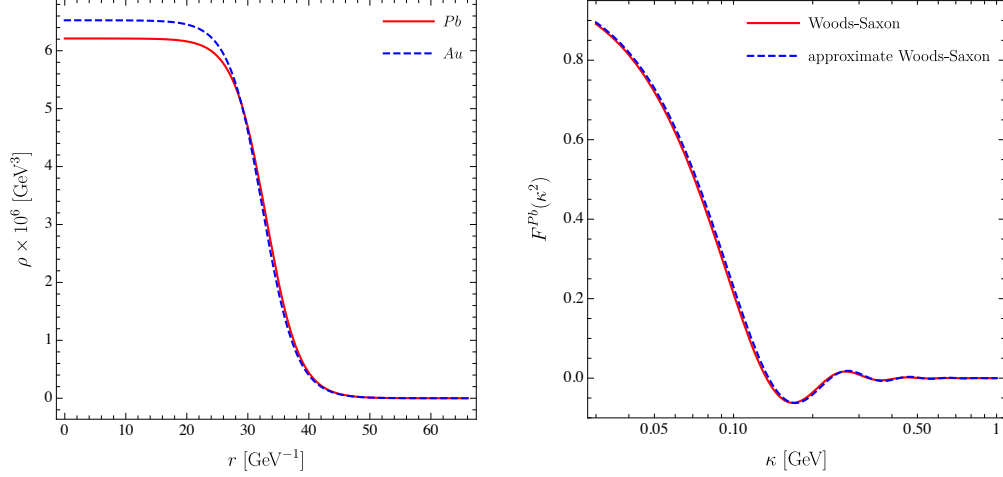


Figure 2. Left: The nuclear charge spatial distribution $\rho(r)$ within the Woods-Saxon model of lead (red solid curve) and gold nuclei (blue dashed curve), both of which have been normalized to unity $\int d^3r \rho(r) = 1$; Right: The lead nuclear charge form factor $F(\kappa^2)$ of the Woods-Saxon type (solid red curve) and from STARlight Monte Carlo event generator (dashed blue curve).

the plot we find that the typical transverse momentum of the photon is about 50 MeV for Pb , and then the corresponding azimuthal angular is too small and can not explain the results observed by the ATLAS collaboration. Therefore we also need to systematically calculate higher-order QCD and QED corrections in order to describe data at the LHC. In the following section we will consider the all-order resummation corrections from final-state QCD radiations, which plays a dominant role for jet production, and we leave a full QCD and QED showers study for the future work.

3 Factorization and resummation for final-state radiations

In this section we will present the resummation formula describing final-state QCD emissions from the dijet system, which contributes the azimuthal decorrelation of the dijet pair. In order to obtain such formalism, we first apply SCET to write down a factorized formula, and express the differential cross section as the product of single scale key ingredients at leading power. Based on the factorization formula and requirements of the factorization scale independence for the cross section, we obtain the all-order resummation formula via solving corresponding renormalization group (RG) equations.

Before introducing our methodology, we first briefly describe two methods on the market used to perform resummation of large logarithms of the azimuthal angle for jets [45–59]. The first method is deriving an all-order resummation formula for the transverse momentum imbalance q_T , and then constructing the azimuthal decorrelation $\Delta\phi$ distribution from the q_T distribution, which can be named as the “indirect method”. The second method is calculating the resummed results of the azimuthal angular distribution directly, so we name it as the “direct method”. The relation between two methods is obvious for Drell-Yan-like processes, but for the scattering processes involving jet production it is not easy to estab-

lish the relation, since one also needs to carry out the resummation of large logarithms from final-state QCD radiations. As shown in [52, 68, 69], in the indirect method the single logarithmic anomalous dimensions of the soft and collinear-soft function with the narrow cone approximation both depend on the azimuthal angle of \mathbf{q}_T (or the azimuthal angle of \mathbf{b} in the Fourier conjugate transverse coordinate space). After taking into account QCD evolution, this azimuthal integral is divergent in some phase space region. In order to regularize such divergences, different schemes have been proposed in [52, 68, 70]. In this paper we consider QCD resummation of large logarithms of azimuthal angle and jet radius at the NLL accuracy. Therefore, in order to avoid such difficulties, we will apply the direct method in the latter calculations.

3.1 QCD factorization formalism in SCET

A factorization formula for the boson-jet azimuthal decorrelation has been comprehensively derived by one of us in [56] within SCET, for the case where jets are defined using the anti- k_T algorithm [71] with the p_T^n -weighted recombination scheme. Although in this paper we consider the jet definition using the standard recombination schemes, which is different from p_T^n -weighted scheme, the factorization formula still share many similar properties. Therefore, we only present main features of the factorized structure, and a more detailed discussion on the factorization analysis within SCET can be found in [56].

At the first step, we use scaling arguments to identify the regions of phase space that contributes to the factorization formula at the leading power. In the back-to-back limit where $\Delta\phi_{jj} \rightarrow \pi$, the relevant low energy modes for the factorized expression in SCET are given by

$$\textcolor{blue}{n_i \text{ collinear}} : p_{c_i}^\mu \sim p_T (R^2, 1, R)_{n_i \bar{n}_i}, \quad (3.1)$$

$$\textcolor{teal}{n_i \text{ collinear-soft}} : p_{cs_i}^\mu \sim \frac{p_T \delta\phi}{R} (R^2, 1, R)_{n_i \bar{n}_i}, \quad (3.2)$$

$$\textcolor{red}{\text{soft}} : p_s^\mu \sim p_T (\delta\phi, \delta\phi, \delta\phi), \quad (3.3)$$

with $\delta\phi \equiv \pi - \Delta\phi_{jj}$. Here all the momenta $p^\mu \equiv (n_i \cdot p, \bar{n}_i \cdot p, p_{n_i \perp})_{n_i \bar{n}_i}$ are expressed using light-cone coordinates, where n_1^μ and n_2^μ are light-like vectors along leading and sub-leading jets, separately, and \bar{n}_i^μ is the direction backwards to the jet. In the above analysis we have considered the limits $R \ll 1$, therefore the narrow cone approximation as well. As a result, the n_i collinear mode (3.1) describes energetic emissions inside the jet with radius R , which only contributes to the normalization of the $\Delta\phi_{jj}$ -distribution, not to its shape. While both n_i collinear-soft and soft mode contribute to $\Delta\phi_{jj}$ -distribution, where $p_{cs_i}^\mu$ is sensitive to the jet boundary but p_s^μ is not. Besides, the soft mode describes large-angle radiations without any direction preference, so in (3.3) the subscript of p_s^μ in light-cone coordinates can be ignored.

With the relevant scaling identified, we can write down a factorized form for the differential cross section at the leading power of $\delta\phi$

$$\frac{d^4\sigma}{dq_x dp_T dy_1 dy_2} = \int dk_x d\lambda_x dl_{1,x} dl_{2,x} \delta(q_x + \lambda_x + l_{1,x} + l_{2,x} - k_x) B(k_x, p_T, y_1, y_2)$$

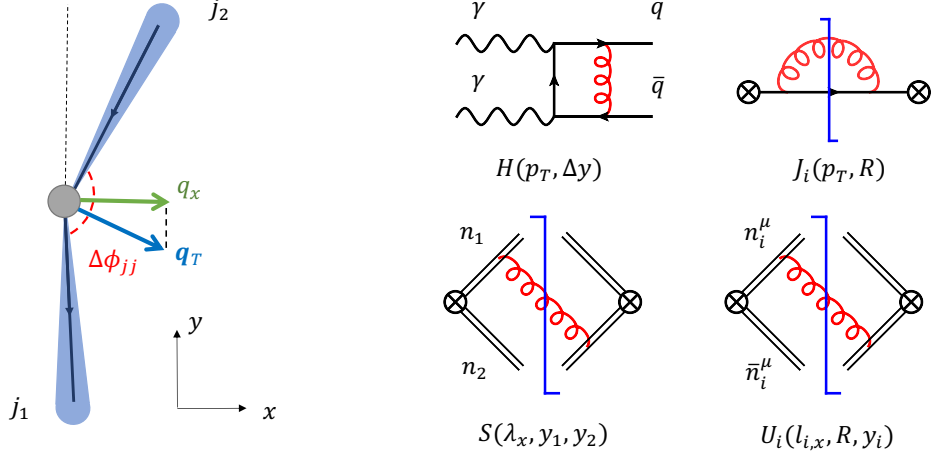


Figure 3. Left: The definition of the azimuthal angle $\Delta\phi_{jj}$ between leading jet j_1 and subleading jet j_2 in x - y plane, and the relation between $\Delta\phi_{jj}$ and momentum q_x in the factorized formula (3.4), where \mathbf{q}_T is the vector sum of the transverse momenta for the dijet, and q_x is the projection of \mathbf{q}_T in the x -axis. Right: Sample one-loop diagrams of the hard, jet, soft as well as collinear-soft functions in (3.4).

$$\begin{aligned} & \times H(p_T, \Delta y, \mu) S(\lambda_x, y_1, y_2, \mu, \nu) U_1(l_{1,x}, R, y_1, \mu, \nu) J_1(p_T, R, \mu) \\ & \times U_2(l_{2,x}, R, y_2, \mu, \nu) J_2(p_T, R, \mu), \end{aligned} \quad (3.4)$$

with $|q_x| \approx p_T \sin(\pi - \Delta\phi_{jj}) = p_T \sin \delta\phi$ as shown in the left panel of figure 3, where we take the leading jet's transverse momentum as reference for $-y$ direction,

$$\mathbf{p}_{1T} \approx (0, -p_T), \quad \mathbf{p}_{2T} \approx p_T(\sin \delta\phi, \cos \delta\phi). \quad (3.5)$$

In (3.4) the Dirac delta function term in the first line indicates the momentum conservation of different ingredients along x -axis, neglecting power corrections. Explicitly, the pieces of the factorized formula (3.4) are:

- $B(k_x, p_T, y_1, y_2)$ is the Born cross section of the process $\gamma\gamma \rightarrow q\bar{q}$ calculated in section 2, and k_x indicates x component of the transverse momentum from incoming photon beams. Explicitly, we obtain the function $B(k_x, p_T, y_1, y_2)$ from (2.2) as

$$B(k_x, p_T, y_1, y_2) = \int dk_y \frac{d^5\sigma_0}{d^2\mathbf{k}_T dp_T dy_1 dy_2}, \quad \text{with } \mathbf{k}_T = (k_x, k_y). \quad (3.6)$$

- $H(p_T, \Delta y)$ is the hard function which can be determined order-by-order in perturbation theory by a matching calculation in QCD and in SCET at the hard scale μ_h . Here $\Delta y \equiv y_1 - y_2$, is defined as the rapidity difference between leading and sub-leading jets.
- $J_i(p_T, R)$ is the jet function describing the emission of collinear radiations inside the anti- k_T jet with radius R , and its mode has momenta that scale as $p_{c_i}^\mu$.

- $U_i(l_{i,x}, R, y_i)$ is the collinear-soft function describing the soft radiation along the direction of the jet, and it is sensitive to the jet direction and the jet boundary. In addition, the collinear-soft mode $p_{cs_i}^\mu$ can also resolve any possible collinear constituents of the jet, which can give the so-called NGLs, as discussed in the following paragraph.
- $S(\lambda_x, y_1, y_2)$ is the transverse momentum dependent soft function which integrates the radiation from the leading and sub-leading jets, so it depends on the rapidity of jets explicitly.

Their one-loop sample diagrams in SCET are given in the right panel of figure 3, and in the appendix A we present the explicit calculations of the soft and collinear-soft functions at one loop. In addition to the factorization scale μ dependence, we also present the soft S and collinear-soft U_i functions with explicit rapidity scale ν dependence, which stems from rapidity divergence and the corresponding regulator. In the following subsection we will apply the collinear anomaly formalism in [72, 73] to resum corresponding rapidity logarithms. Alternatively, it can be dealt with using the rapidity renormalization group method [74, 75]. Finally, it should be noted that the above factorized expression (3.4) has ignored the structure from non-global logarithms (NGLs), which start contributing at two-loop order [60]. The TMD factorization formula including those effects have been discussed in [51, 52, 76], and one finds that NGLs can be resummed via a fitting function given in [60] at NLL level. In our phenomenology, we have included their contributions in the resummation formula.

After performing Fourier transform for (3.4), we obtain the factorized formula in the coordinate space as follows

$$\begin{aligned} \frac{d^4\sigma}{dq_x dp_T dy_1 dy_2} &= \int_{-\infty}^{+\infty} \frac{db_x}{2\pi} e^{iq_x b_x} \tilde{B}(b_x, p_T, y_1, y_2) H(p_T, \Delta y, \mu) \tilde{S}(b_x, y_1, y_2, \mu, \nu) \\ &\quad \times \tilde{U}_1(b_x, R, y_1, \mu, \nu) J_1(p_T, R, \mu) \tilde{U}_2(b_x, R, y_2, \mu, \nu) J_2(p_T, R, \mu), \end{aligned} \quad (3.7)$$

where \tilde{B} , \tilde{S} and \tilde{U}_i are the Fourier transform of B , S and U_i in (3.4), respectively. Except the Born cross section \tilde{B} , all other ingredients are normalized to 1 at the leading order. Accordingly, as a check one can easily see that at the leading order the above formula (3.7) degenerate (2.2) for the quark-antiquark pairs production without final-state radiations.

3.2 QCD resummation formalism of final-state radiation

In this section, we present the RG equations for the factorization scale dependent ingredients in (3.7), including the hard function H , jet function J_i , soft function \tilde{S} , and collinear-soft function \tilde{U}_i . After presenting their RG evolution equations, we check the RG consistency at one loop. In the end, we present the all-order QCD resummation formula for the azimuthal angular distribution.

For the hard scattering process $\gamma\gamma \rightarrow q\bar{q}$, the QCD corrections have been perturbatively calculated at three loop [77], and the corresponding RG equation of the hard function reads

$$\frac{d}{d\ln\mu} H(p_T, \Delta y, \mu) = \underbrace{\left[-2C_F\gamma_{\text{cusp}}(\alpha_s) \ln \frac{\mu^2}{M^2} + 4\gamma_q(\alpha_s) \right]}_{\equiv \Gamma_H(\alpha_s)} H(p_T, \Delta y, \mu), \quad (3.8)$$

where we have defined the hard anomalous dimension $\Gamma_H(\alpha_s)$, and M is the invariant mass of dijet pair defined in (2.4). In the appendix B we present the perturbative expression of all relevant anomalous dimensions for the NLL resummation.

The one-loop quark jet function for the anti- k_T algorithm with radius R is calculated in [78], and it satisfies the RG evolution equations

$$\frac{d}{d\ln\mu} J_i(p_T, R, \mu) = \underbrace{\left[-C_F\gamma_{\text{cusp}}(\alpha_s) \ln \frac{p_T^2 R^2}{\mu^2} - 2\gamma_q(\alpha_s) \right]}_{\equiv \Gamma_J(\alpha_s)} J_i(p_T, R, \mu). \quad (3.9)$$

From (3.8) and (3.9) one can see that the characteristic scales related to the hard and jet functions would be $\mu_h \sim M$ and $\mu_j \sim p_T R$, respectively.

Due to the existence of rapidity divergences, the calculation of soft and collinear-soft functions involves extra complication which is not seen in the calculation of the hard and jet functions. In appendix A we present their one-loop calculations in (A.1) and (A.3), where we introduce a rapidity regulator by modifying the phase-space integrals [79].

$$\int d^d k \rightarrow \int d^d k \left(\frac{\nu}{2k^0} \right)^\eta. \quad (3.10)$$

Such divergences are artificial because the product of the soft and collinear-soft functions is independent on the scale ν . However, the rapidity divergence introduces additional logarithmic dependence of the jet radius R , so (3.7) does not achieve complete factorization. By refactorizing out R -dependence terms within the collinear anomaly framework [72, 73], the product of soft and collinear-soft functions should be expressed as

$$\tilde{U}_1(b, R, y_1, \mu, \nu) \tilde{U}_2(b, R, y_2, \mu, \nu) \tilde{S}(b, y_1, y_2, \mu, \nu) = R^{2F_{q\bar{q}}(b, \mu)} W(b, \Delta y, \mu), \quad (3.11)$$

where the reminder function $W(b, \Delta y, \mu)$ no longer contains large logarithms of the jet radius, and the relevant R -dependent logarithms are resummed by the help of the anomaly exponent $F_{q\bar{q}}(b, \mu)$. Explicitly, their one-loop expressions are given by

$$F_{q\bar{q}}(b, \mu) = \frac{\alpha_s}{4\pi} C_F \gamma_0^{\text{cusp}} \ln \frac{b^2 \mu^2}{b_0^2} + \mathcal{O}(\alpha_s^2), \quad (3.12)$$

$$W(b, \Delta y, \mu) = 1 - \frac{\alpha_s}{4\pi} C_F \left[\gamma_0^{\text{cusp}} \ln(2 + 2 \cosh \Delta y) \ln \frac{b^2 \mu^2}{b_0^2} \right] + \mathcal{O}(\alpha_s^2), \quad (3.13)$$

where the reminder function W is normalized to 1 at the leading order, and they satisfy the following RG equations:

$$\frac{d}{d\ln\mu} F_{q\bar{q}}(b, \mu) = 2C_F \gamma_{\text{cusp}}(\alpha_s), \quad (3.14)$$

$$\frac{d}{d \ln \mu} W(b, \Delta y, \mu) = \left[-2C_F \gamma_{\text{cusp}}(\alpha_s) \ln(2 + 2 \cosh \Delta y) \right] W(b, \Delta y, \mu). \quad (3.15)$$

In appendix A we present the one-loop calculation of the soft and collinear-soft functions, and one can easily verify that the rapidity poles are cancelled in the product of \tilde{S} and \tilde{U}_i , and also reproduce the refactorization formula (3.11).

With the anomalous dimensions presented for all the ingredients, one can easily verify that the factorized formula given in (3.7) satisfies the consistency relations for the RG evolution

$$\frac{d}{d \ln \mu} \left[R^{2F_{q\bar{q}}(b, \mu)} W(b, \Delta y, \mu) H(p_T, \Delta y, \mu) J_1(p_T, R, \mu) J_2(p_T, R, \mu) \right] = 0. \quad (3.16)$$

In the end all large logarithms can be resummed by evolving the hard and jet functions from their intrinsic scales μ_h and μ_j to the scale of the reminder function and the anomaly exponent at μ_b separately, and at NLL accuracy we have

$$\begin{aligned} \frac{d^4 \sigma^{\text{NLL}}}{dq_x dp_T dy_1 dy_2} &= \int_0^\infty \frac{db_x}{\pi} \cos(q_x b_x) \tilde{B}(b_x, p_T, y_1, y_2) \\ &\times \exp \left[\int_{\mu_h}^{\mu_b} \frac{d\mu}{\mu} \Gamma_H(\alpha_s) + 2 \int_{\mu_j}^{\mu_b} \frac{d\mu}{\mu} \Gamma_J(\alpha_s) \right] U_{\text{NG}}^2(\mu_b, \mu_j), \end{aligned} \quad (3.17)$$

where we have incorporated NGLs resummation effects included by the function U_{NG} . As shown in [51, 52, 76] the fitting function given in [60] can be used to capture leading-logarithmic NGLs after choosing proper initial and final evolution scales. In our process, the resummation of NGLs comes from a non-linear RG evolution between the jet and the collinear-soft function [52], so we choose the jet scale μ_j and μ_b for the reminder function in the function U_{NG} that is given by

$$U_{\text{NG}}(\mu_b, \mu_j) = \exp \left[-C_A C_F \frac{\pi^2}{3} u^2 \frac{1 + (au)^2}{1 + (bu)^c} \right], \quad (3.18)$$

with $a = 0.85 C_A$, $b = 0.86 C_A$, $c = 1.33$ and $u = \ln[\alpha_s(\mu_b)/\alpha_s(\mu_j)]/\beta_0$. Since there are two jet functions in the factorized formula (3.7), we need to include the square of U_{NG} to take into account the NGL resummation associated with each jet.

4 Numerical results

In this section we will present the numerical results using the resummation formula (3.17), which captures both non-zero transverse momentum from incoming photons and QCD evolution of final-state radiations at NLL accuracy.

We see that, after the change of integration variable from q_x to $\Delta\phi_{jj}$ in (3.17), the theoretical results for $\Delta\phi_{jj}$ -distribution can be directly obtained where we choose the intrinsic scales in the resummation formula as

$$\mu_h = M, \quad \mu_j = p_T R, \quad \mu_b = \frac{b_0}{b_*(b_x)}. \quad (4.1)$$

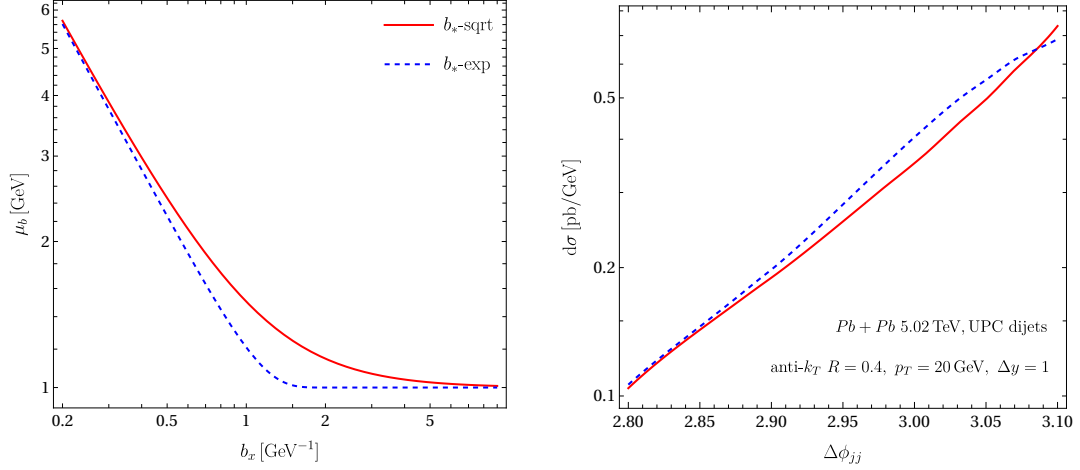


Figure 4. Left: The scale μ_b in (4.1) depending on the functional form chosen for b_* : the red solid line is obtained with the square-root form, while the blue dashed line with the exponential form; see (4.2) and (4.3). Right: Uncertainties of the differential cross section estimated by varying the functional forms in the b_* -prescription. In both cases we choose $b_{\max} = 1.123 \text{ GeV}^{-1}$.

In the above expressions, we introduce a function $b_*(b_x)$ to freeze the value of μ_b in the non-perturbative region as $b_x \rightarrow \infty$, since pQCD calculations will hit the Landau pole. The standard “square-root form” [80] of this function is defined as

$$b_*(b) = \frac{b}{\sqrt{1 + b^2/b_{\max}^2}}. \quad (4.2)$$

In order to estimate the corresponding theoretical uncertainties from different function forms, we also present the result using the “exponential form” [81]

$$b_*(b) = b_{\max} [1 - \exp(-b^4/b_{\max}^4)]^{1/4}. \quad (4.3)$$

to avoid the Landau pole. By introducing the function $b_*(b_x)$, one has $\mu_b \sim b_0/b_x$ when $b_x \ll b_{\max}$, and $\mu_b \sim b_0/b_{\max}$ when $b_x \gg b_{\max}$, as is shown in the left panel of figure 4, where the solid red and dashed blue curves are the scales μ_b with square-root and exponential form, respectively. In both cases, we choose the scale μ_b freeze at 1 GeV as $b_x \rightarrow \infty$. As expected, these two forms have the same asymptotic behaviors in both large b_x and small b_x regions. The right panel of figure 4 shows that these two forms lead to similar predictions for the differential cross section in (3.17). From the figure, we find that as $\Delta\phi_{jj} \sim \pi$ the sensitivity of our predictions to this function form is about 10%, and when $\Delta\phi_{jj} < 2.9$ it has a negligible effect on numerics, where we choose $p_T = 20 \text{ GeV}$ and $\Delta y = 1$. Since the uncertainty from different function forms is smaller than that from the scale variation, in the rest of this paper we will use the standard “square-root form” in (4.2).

In the end we will compare our theoretical calculation of the azimuthal angular decorrelation $\Delta\phi_{jj}$ with the experimental results in [22], where we only consider the kinematic region where the jet pair is produced nearly back to back. In this region the contribution

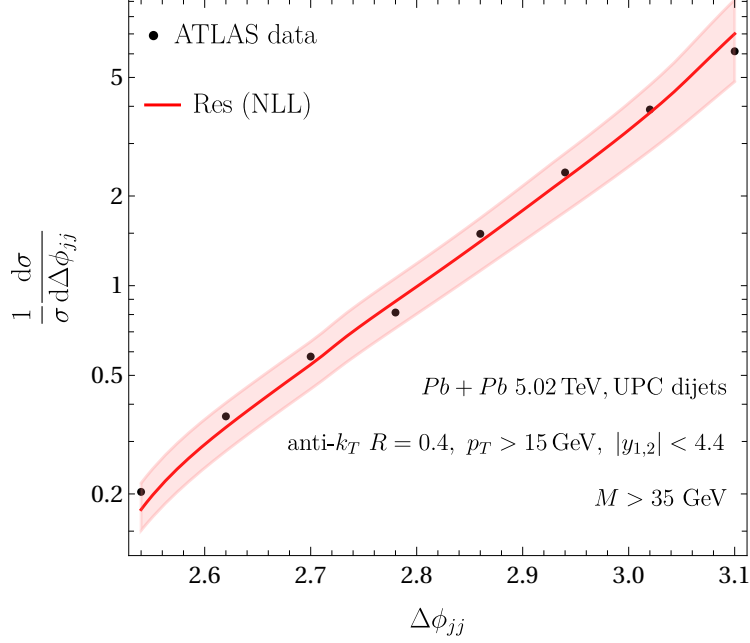


Figure 5. Comparison between theoretical calculations of the azimuthal decorrelation with the preliminary ATLAS data [22], where $\Delta\phi_{jj}$ is the azimuthal angle between two jets with highest transverse momenta. The theoretical and experimental distributions are normalised such that the area under the curve is equal to 1. The black dots are the ATLAS results, and the uncertainties of the data are smaller than the symbol size used in the plot. The solid red curve is the result with the scale choice in (4.1), and the theoretical uncertainty for the red band is obtained from the variation of scales in the resummation formula.

from multijets production are power suppressed, and we leave fixed-order pQCD calculations of multijets production for future studies.¹ In order to make a comparison, we calculate (3.17) with the same kinematic cuts as in [22]

$$p_T > 15 \text{ GeV}, \quad |y_{1,2}| < 4.4, \quad M > 35 \text{ GeV}, \quad (4.4)$$

and the jet radius $R = 0.4$. As is shown in figure 5 the red curve is the theoretical predictions with the scale choice in (4.1), and the error bands are shown as the shaded regions where we consider the theoretical uncertainty from the scales. Specifically, we perform a variation of μ_h , μ_j and μ_b scales by a factor of 2 about the central values, and then combine these uncertainties by taking the envelope. The black dots are the ATLAS results, where we find experimental errors are small and can hardly be seen in the plot. The theoretical and experimental distributions are normalised such that the area under the curve is equal to 1. From the plot it is clear to see that our result is consistent with the experimental data.

¹Very recently, a new phenomenological code for automated fixed-order calculations of the photon-induced processes in UPCs is presented in [82].

5 Conclusion

In this paper we study the azimuthal decorrelation of dijet productions from photon-photon fusions in UPCs, where the dijet is produced nearly back-to-back in the transverse plane with respect to the beam direction. We calculate the key measurement, acoplanarity distribution, which is the distribution of the azimuthal angle $\Delta\phi_{jj}$ between the leading and the subleading jet. The azimuthal decorrelation is produced via both the non-trivial transverse momentum distribution of the incoming photon flux and QCD radiations from the outgoing partons, which leads to the factorized formula (3.4), namely the convolution of the initial state and the final state. The initial quark-antiquark pairs production is performed by the hard scattering of the diphoton associated with the EPA photon spectrum. In addition, the final-state radiations are described by the factorization and resummation formula at NLL accuracy within the SCET framework.

We vary the scales in resummation formula and obtain a theoretical band of the normalized acoplanarity distribution. Figure 5 shows a good agreement with the ATLAS experimental data in the nearly back-to-back region, where we note that the PYTHIA8 Monte Carlo event generator simulates a noticeably narrower $\Delta\phi_{jj}$ distribution compared to the data [22]. However, both our theoretical calculations and the PYTHIA8 simulation severely underpredict the total cross section of the experiment (roughly by a factor of 10), which implies some missing progresses (e.g. diffractive dijet photoproductions) in these UPC $0n0n$ events to be studied in the future. We argue that these additional dijet photoproductions may enhance the dijet production yields, but should barely change the azimuthal angular distribution shape since it is dominated by the final-state radiations.

Acknowledgments

C.Z. is supported by the National Science Foundations of China under Grant No. 12147125. D.Y.S. is supported by the National Science Foundations of China under Grant No. 12275052 and the Shanghai Natural Science Foundation under Grant No. 21ZR1406100.

A Soft, collinear-soft functions and the collinear anomaly

The operator definition of the soft function can be found in [56], and here we summarize its one-loop results. The NLO soft function reads

$$\begin{aligned} \tilde{S}(b_x, y_1, y_2, \mu, \nu) &= 1 + 2 C_F g_s^2 \tilde{\mu}^{2\epsilon} \int \frac{d^d k}{(2\pi)^{d-1}} \delta(k^2) \theta(k^0) \left(\frac{\nu}{2k^0} \right)^\eta \frac{n_1 \cdot n_2}{n_1 \cdot k k \cdot n_2} e^{-ib_x k_x} \\ &= 1 + \frac{\alpha_s}{4\pi} C_F \left[- \left(\frac{2}{\eta} + \ln \frac{\nu^2 n_1 \cdot n_2}{2\mu^2} \right) \left(\frac{4}{\epsilon} + 4 \ln \frac{\mu^2 b_x^2}{b_0^2} \right) + \frac{4}{\epsilon^2} - 2 \ln^2 \frac{\mu^2 b_x^2}{b_0^2} - \frac{\pi^2}{3} \right], \quad (\text{A.1}) \end{aligned}$$

with $\tilde{\mu}^2 = \mu^2 e^{\gamma_E} / (4\pi)$ and $b_0 = 2e^{-\gamma_E}$. Here the rapidity regulator is given in (3.10). In order to evaluate the one-loop collinear-soft function U_i , it is convenient to expand the integrated momentum k^μ along the light-like reference vector n_i^μ . Explicitly, we have

$$k^\mu = \frac{n_i^\mu}{2} \bar{n}_i \cdot k + \frac{\bar{n}_i^\mu}{2} n_i \cdot k + k_\perp^\mu. \quad (\text{A.2})$$

Then the one-loop collinear-soft function is written as

$$\begin{aligned}
\tilde{U}_i(b_\perp, y_i, \mu, \nu) &= 1 + 2 C_F g_s^2 \tilde{\mu}^{2\epsilon} \int \frac{d^d k}{(2\pi)^{d-1}} \delta(k^2) \theta(k^0) \left(\frac{\nu}{\bar{n}_i \cdot k} \right)^\eta \frac{n_i \cdot \bar{n}_i}{n_i \cdot k k \cdot \bar{n}_i} \\
&\times \left\{ e^{-i b_\perp \cdot k_\perp \theta} \left[\frac{n_i \cdot k}{\bar{n}_i \cdot k} - \left(\frac{R}{2 \cosh y_i} \right)^2 \right] + \theta \left[\left(\frac{R}{2 \cosh y_i} \right)^2 - \frac{n_i \cdot k}{\bar{n}_i \cdot k} \right] \right\} \\
&= 1 + \frac{\alpha_s}{4\pi} C_F \left[\left(\frac{2}{\eta} + \ln \frac{\nu^2 R^2}{4\mu^2 \cosh^2 y_i} \right) \left(\frac{2}{\epsilon} + 2 \ln \frac{\mu^2 b_\perp^2}{b_0^2} \right) - \frac{2}{\epsilon^2} + \ln^2 \frac{\mu^2 b_\perp^2}{b_0^2} + \frac{\pi^2}{6} \right], \quad (\text{A.3})
\end{aligned}$$

where the rapidity regulator is also expanded at the leading power as suggested in (3.2). The collinear-soft mode describes low energy radiations emitted from the collinear partons in the jet at an angle $\theta \sim R$, and the step functions in the second line indicate that only emissions outside the jet contribute to transverse momentum imbalance at one loop.

As shown in (3.11), after combining soft and collinear-soft functions the jet radius dependence would be factorized out. At order α_s , using (A.1) and (A.3), we find

$$\begin{aligned}
\tilde{S}(b_x, y_1, y_2, \mu, \nu) \tilde{U}_1(b_x, y_1, \mu, \nu) \tilde{U}_2(b_x, y_2, \mu, \nu) \\
= 1 + C_F \frac{\alpha_s}{\pi} \left[\ln R^2 - \ln(2 + 2 \cosh \Delta y) \right] \left(\frac{1}{\epsilon} + \ln \frac{b_x^2 \mu^2}{b_0^2} \right) + \mathcal{O}(\alpha_s^2), \quad (\text{A.4})
\end{aligned}$$

where the poles in η and scale ν dependence in the NLO terms cancel out. Since we consider $R \ll 1$ in (3.7), the logarithm of R indicates that a complete separation of scales was not achieved. In order to carry out the resummation of the logarithmic of the jet radius R , one obtain the refactorized formula in (3.11). At one-loop order we find $\overline{\text{MS}}$ renormalized result of (A.4) agrees with (3.11) using the exponent $F_{q\bar{q}}$ in (3.12) and the reminder function W in (3.13).

In the above calculation we evaluate both of the one-loop soft and collinear-soft functions in the lab frame where rapidities $y_{1,2}$ of dijet are arbitrary, and obtain general expansions of them. However, since the product of the soft and the collinear-soft functions are boost invariant along the beam axis as given in (3.7), they can also be simultaneously calculated in the center-of-mass frame of two incoming photons, which would gives the same result as in (A.4) after combining them together.

B Anomalous dimension

The QCD β -function and the cusp and non-cusp anomalous dimensions in the $\overline{\text{MS}}$ renormalization scheme are expanded as

$$\beta(\alpha_s) = -2\alpha_s \sum_{n=0}^{\infty} \beta_n \left(\frac{\alpha_s}{4\pi} \right)^{n+1}, \quad \gamma(\alpha_s) = \sum_{n=0}^{\infty} \gamma_n \left(\frac{\alpha_s}{4\pi} \right)^{n+1}. \quad (\text{B.1})$$

The two-loop coefficients of the β -function and the cusp anomalous dimensions, and the one-loop coefficient of the non-cusp anomalous dimensions read,

$$\beta_0 = \frac{11}{3} C_A - \frac{4}{3} T_F n_f, \quad \beta_1 = \frac{34}{3} C_A^2 - \frac{20}{3} T_F C_A n_f - 4 T_F C_F n_f, \quad (\text{B.2})$$

$$\gamma_0^{\text{cusp}} = 4, \quad \gamma_1^{\text{cusp}} = \left(\frac{268}{9} - \frac{4\pi^2}{3} \right) C_A - \frac{80}{9} T_F n_f, \quad \gamma_0^q = -3C_F, \quad (\text{B.3})$$

with $T_F = 1/2$, $C_A = 3$, $C_F = 4/3$, $n_f = 5$.

References

- [1] ZEUS collaboration, S. Chekanov et al., *Exclusive photoproduction of J/ψ mesons at HERA*, *Eur. Phys. J. C* **24** (2002) 345–360, [[hep-ex/0201043](#)].
- [2] PHENIX collaboration, S. Afanasiev et al., *Photoproduction of J/ψ and of high mass e^+e^- in ultra-peripheral Au+Au collisions at $\sqrt{s} = 200 \text{ GeV}$* , *Phys. Lett. B* **679** (2009) 321–329, [[0903.2041](#)].
- [3] ALICE collaboration, J. G. Contreras, *Photoproduction of J/ψ in Pb-Pb and p-Pb collisions at the LHC with the ALICE detector*, *EPJ Web Conf.* **60** (2013) 13007.
- [4] STAR collaboration, W. Schmidke, *J/ψ Production in Ultra-Peripheral Collisions at STAR*, *PoS DIS2016* (2016) 189.
- [5] CMS collaboration, V. Khachatryan et al., *Coherent J/ψ photoproduction in ultra-peripheral PbPb collisions at $\sqrt{s_{\text{NN}}} = 2.76 \text{ TeV}$ with the CMS experiment*, *Phys. Lett. B* **772** (2017) 489–511, [[1605.06966](#)].
- [6] ALICE collaboration, S. Acharya et al., *Coherent J/ψ photoproduction at forward rapidity in ultra-peripheral Pb-Pb collisions at $\sqrt{s_{\text{NN}}} = 5.02 \text{ TeV}$* , *Phys. Lett. B* **798** (2019) 134926, [[1904.06272](#)].
- [7] ALICE collaboration, S. Acharya et al., *First measurement of the $|t|$ -dependence of coherent J/ψ photonuclear production*, *Phys. Lett. B* **817** (2021) 136280, [[2101.04623](#)].
- [8] LHCb collaboration, R. Aaij et al., *Study of coherent J/ψ production in lead-lead collisions at $\sqrt{s_{\text{NN}}} = 5 \text{ TeV}$* , *JHEP* **07** (2022) 117, [[2107.03223](#)].
- [9] STAR collaboration, M. Abdallah et al., *Probing the Gluonic Structure of the Deuteron with J/ψ Photoproduction in d+Au Ultraperipheral Collisions*, *Phys. Rev. Lett.* **128** (2022) 122303, [[2109.07625](#)].
- [10] STAR collaboration, M. Abdallah et al., *Tomography of Ultra-relativistic Nuclei with Polarized Photon-gluon Collisions*, [2204.01625](#).
- [11] S. J. Brodsky, L. Frankfurt, J. F. Gunion, A. H. Mueller and M. Strikman, *Diffraction leptoproduction of vector mesons in QCD*, *Phys. Rev. D* **50** (1994) 3134–3144, [[hep-ph/9402283](#)].
- [12] S. Klein and J. Nystrand, *Exclusive vector meson production in relativistic heavy ion collisions*, *Phys. Rev. C* **60** (1999) 014903, [[hep-ph/9902259](#)].
- [13] H. Kowalski, L. Motyka and G. Watt, *Exclusive diffractive processes at HERA within the dipole picture*, *Phys. Rev. D* **74** (2006) 074016, [[hep-ph/0606272](#)].
- [14] V. Rebyakova, M. Strikman and M. Zhalov, *Coherent ρ and J/ψ photoproduction in ultraperipheral processes with electromagnetic dissociation of heavy ions at RHIC and LHC*, *Phys. Lett. B* **710** (2012) 647–653, [[1109.0737](#)].
- [15] T. Lappi and H. Mantysaari, *J/ψ production in ultraperipheral Pb+Pb and p+Pb collisions at energies available at the CERN Large Hadron Collider*, *Phys. Rev. C* **87** (2013) 032201, [[1301.4095](#)].

- [16] V. Guzey and M. Zhalov, *Exclusive J/ψ production in ultraperipheral collisions at the LHC: constraints on the gluon distributions in the proton and nuclei*, *JHEP* **10** (2013) 207, [[1307.4526](#)].
- [17] Y.-p. Xie and X. Chen, *The coherent cross section of vector mesons in ultraperipheral PbPb collisions at the LHC*, *Eur. Phys. J. C* **76** (2016) 316, [[1602.00937](#)].
- [18] H. Xing, C. Zhang, J. Zhou and Y.-J. Zhou, *The $\cos 2\phi$ azimuthal asymmetry in ρ^0 meson production in ultraperipheral heavy ion collisions*, *JHEP* **10** (2020) 064, [[2006.06206](#)].
- [19] W. Zha, J. D. Brandenburg, L. Ruan, Z. Tang and Z. Xu, *Exploring the double-slit interference with linearly polarized photons*, *Phys. Rev. D* **103** (2021) 033007, [[2006.12099](#)].
- [20] J. D. Brandenburg, Z. Xu, W. Zha, C. Zhang, J. Zhou and Y. Zhou, *Exploring gluon tomography with polarization dependent diffractive J/ψ production*, [2207.02478](#).
- [21] H. Mäntysaari, F. Salazar and B. Schenke, *Nuclear geometry at high energy from exclusive vector meson production*, [2207.03712](#).
- [22] ATLAS collaboration, *Photo-nuclear jet production in ultra-peripheral Pb+Pb collisions at $\sqrt{s_{NN}} = 5.02$ TeV with the ATLAS detector*, .
- [23] STAR collaboration, J. Adams et al., *Production of e^+e^- pairs accompanied by nuclear dissociation in ultra-peripheral heavy ion collision*, *Phys. Rev. C* **70** (2004) 031902, [[nucl-ex/0404012](#)].
- [24] STAR collaboration, J. Adam et al., *Low- p_T e^+e^- pair production in Au+Au collisions at $\sqrt{s_{NN}} = 200$ GeV and U+U collisions at $\sqrt{s_{NN}} = 193$ GeV at STAR*, *Phys. Rev. Lett.* **121** (2018) 132301, [[1806.02295](#)].
- [25] STAR collaboration, J. Adam et al., *Measurements of Dielectron Production in Au+Au Collisions at $\sqrt{s_{NN}} = 27, 39$, and 62.4 GeV from the STAR Experiment*, [1810.10159](#).
- [26] ATLAS collaboration, M. Aaboud et al., *Observation of centrality-dependent acoplanarity for muon pairs produced via two-photon scattering in Pb+Pb collisions at $\sqrt{s_{NN}} = 5.02$ TeV with the ATLAS detector*, *Phys. Rev. Lett.* **121** (2018) 212301, [[1806.08708](#)].
- [27] ALICE collaboration, S. Acharya et al., *Measurement of dielectron production in central Pb-Pb collisions at $\sqrt{s_{NN}} = 2.76$ TeV*, *Phys. Rev. C* **99** (2019) 024002, [[1807.00923](#)].
- [28] ATLAS collaboration, G. Aad et al., *Exclusive dimuon production in ultraperipheral Pb+Pb collisions at $\sqrt{s_{NN}} = 5.02$ TeV with ATLAS*, *Phys. Rev. C* **104** (2021) 024906, [[2011.12211](#)].
- [29] ATLAS collaboration, M. Aaboud et al., *Evidence for light-by-light scattering in heavy-ion collisions with the ATLAS detector at the LHC*, *Nature Phys.* **13** (2017) 852–858, [[1702.01625](#)].
- [30] M. Vidovic, M. Greiner, C. Best and G. Soff, *Impact parameter dependence of the electromagnetic particle production in ultrarelativistic heavy ion collisions*, *Phys. Rev. C* **47** (1993) 2308–2319.
- [31] K. Hencken, D. Trautmann and G. Baur, *Impact parameter dependence of the total probability for the electromagnetic electron - positron pair production in relativistic heavy ion collisions*, *Phys. Rev. A* **51** (1995) 1874–1882, [[nucl-th/9410014](#)].
- [32] F. Krauss, M. Greiner and G. Soff, *Photon and gluon induced processes in relativistic heavy ion collisions*, *Prog. Part. Nucl. Phys.* **39** (1997) 503–564.

- [33] W. Zha, J. D. Brandenburg, Z. Tang and Z. Xu, *Initial transverse-momentum broadening of Breit-Wheeler process in relativistic heavy-ion collisions*, *Phys. Lett. B* **800** (2020) 135089, [[1812.02820](#)].
- [34] S. Klein, A. H. Mueller, B.-W. Xiao and F. Yuan, *Acoplanarity of a Lepton Pair to Probe the Electromagnetic Property of Quark Matter*, *Phys. Rev. Lett.* **122** (2019) 132301, [[1811.05519](#)].
- [35] J. D. Brandenburg, W. Zha and Z. Xu, *Mapping the electromagnetic fields of heavy-ion collisions with the Breit-Wheeler process*, *Eur. Phys. J. A* **57** (2021) 299, [[2103.16623](#)].
- [36] R.-j. Wang, S. Pu and Q. Wang, *Lepton pair production in ultraperipheral collisions*, *Phys. Rev. D* **104** (2021) 056011, [[2106.05462](#)].
- [37] C. Li, J. Zhou and Y.-J. Zhou, *Impact parameter dependence of the azimuthal asymmetry in lepton pair production in heavy ion collisions*, *Phys. Rev. D* **101** (2020) 034015, [[1911.00237](#)].
- [38] C. Li, J. Zhou and Y.-J. Zhou, *Probing the linear polarization of photons in ultraperipheral heavy ion collisions*, *Phys. Lett. B* **795** (2019) 576–580, [[1903.10084](#)].
- [39] R.-j. Wang, S. Lin, S. Pu, Y.-f. Zhang and Q. Wang, *Lepton pair photoproduction in peripheral relativistic heavy-ion collisions*, [2204.02761](#).
- [40] E. Fermi, *On the Theory of the impact between atoms and electrically charged particles*, *Z. Phys.* **29** (1924) 315–327.
- [41] C. F. von Weizsacker, *Radiation emitted in collisions of very fast electrons*, *Z. Phys.* **88** (1934) 612–625.
- [42] E. J. Williams, *Correlation of certain collision problems with radiation theory*, *Kong. Dan. Vid. Sel. Mat. Fys. Med.* **13N4** (1935) 1–50.
- [43] C. Bierlich et al., *A comprehensive guide to the physics and usage of PYTHIA 8.3*, [2203.11601](#).
- [44] V. Guzey and M. Klasen, *Diffraction dijet photoproduction in ultraperipheral collisions at the LHC in next-to-leading order QCD*, *JHEP* **04** (2016) 158, [[1603.06055](#)].
- [45] A. Banfi, M. Dasgupta and Y. Delenda, *Azimuthal decorrelations between QCD jets at all orders*, *Phys. Lett. B* **665** (2008) 86–91, [[0804.3786](#)].
- [46] F. Hautmann and H. Jung, *Angular correlations in multi-jet final states from k_{\perp} -dependent parton showers*, *JHEP* **10** (2008) 113, [[0805.1049](#)].
- [47] P. Sun, C. P. Yuan and F. Yuan, *Soft Gluon Resummations in Dijet Azimuthal Angular Correlations in Hadronic Collisions*, *Phys. Rev. Lett.* **113** (2014) 232001, [[1405.1105](#)].
- [48] P. Sun, C. P. Yuan and F. Yuan, *Transverse Momentum Resummation for Dijet Correlation in Hadronic Collisions*, *Phys. Rev. D* **92** (2015) 094007, [[1506.06170](#)].
- [49] L. Chen, G.-Y. Qin, L. Wang, S.-Y. Wei, B.-W. Xiao, H.-Z. Zhang et al., *Study of Isolated-photon and Jet Momentum Imbalance in pp and PbPb collisions*, *Nucl. Phys.* **B933** (2018) 306–319, [[1803.10533](#)].
- [50] P. Sun, B. Yan, C. P. Yuan and F. Yuan, *Resummation of High Order Corrections in Z Boson Plus Jet Production at the LHC*, [1810.03804](#).
- [51] X. Liu, F. Ringer, W. Vogelsang and F. Yuan, *Lepton-jet Correlations in Deep Inelastic Scattering at the Electron-Ion Collider*, *Phys. Rev. Lett.* **122** (2019) 192003, [[1812.08077](#)].

- [52] Y.-T. Chien, D. Y. Shao and B. Wu, *Resummation of Boson-Jet Correlation at Hadron Colliders*, *JHEP* **11** (2019) 025, [[1905.01335](#)].
- [53] X. Liu, F. Ringer, W. Vogelsang and F. Yuan, *Lepton-jet Correlation in Deep Inelastic Scattering*, *Phys. Rev. D* **102** (2020) 094022, [[2007.12866](#)].
- [54] Y.-T. Chien, R. Rahn, S. Schrijnder van Velzen, D. Y. Shao, W. J. Waalewijn and B. Wu, *Azimuthal angle for boson-jet production in the back-to-back limit*, [2005.12279](#).
- [55] M. I. Abdulhamid et al., *Azimuthal correlations of high transverse momentum jets at next-to-leading order in the parton branching method*, *Eur. Phys. J. C* **82** (2022) 36, [[2112.10465](#)].
- [56] Y.-T. Chien, R. Rahn, D. Y. Shao, W. J. Waalewijn and B. Wu, *Precision boson-jet azimuthal decorrelation at hadron colliders*, [2205.05104](#).
- [57] H. Bouaziz, Y. Delenda and K. Khelifa-Kerfa, *Azimuthal decorrelation between a jet and a Z boson at hadron colliders*, [2207.10147](#).
- [58] H. Yang et al., *Back-to-back azimuthal correlations in Z+jet events at high transverse momentum in the TMD parton branching method at next-to-leading order*, *Eur. Phys. J. C* **82** (2022) 755, [[2204.01528](#)].
- [59] A. B. Martinez and F. Hautmann, *Azimuthal di-jet correlations with parton branching TMD distributions*, in *29th International Workshop on Deep-Inelastic Scattering and Related Subjects*, 8, 2022, [2208.08446](#).
- [60] M. Dasgupta and G. P. Salam, *Resummation of nonglobal QCD observables*, *Phys. Lett. B* **512** (2001) 323–330, [[hep-ph/0104277](#)].
- [61] A. Banfi, G. Marchesini and G. Smye, *Away from jet energy flow*, *JHEP* **08** (2002) 006, [[hep-ph/0206076](#)].
- [62] C. W. Bauer, S. Fleming, D. Pirjol and I. W. Stewart, *An Effective field theory for collinear and soft gluons: Heavy to light decays*, *Phys. Rev.* **D63** (2001) 114020, [[hep-ph/0011336](#)].
- [63] C. W. Bauer and I. W. Stewart, *Invariant operators in collinear effective theory*, *Phys. Lett.* **B516** (2001) 134–142, [[hep-ph/0107001](#)].
- [64] C. W. Bauer, D. Pirjol and I. W. Stewart, *Soft collinear factorization in effective field theory*, *Phys. Rev.* **D65** (2002) 054022, [[hep-ph/0109045](#)].
- [65] C. W. Bauer, S. Fleming, D. Pirjol, I. Z. Rothstein and I. W. Stewart, *Hard scattering factorization from effective field theory*, *Phys. Rev.* **D66** (2002) 014017, [[hep-ph/0202088](#)].
- [66] M. Beneke, A. P. Chapovsky, M. Diehl and T. Feldmann, *Soft collinear effective theory and heavy to light currents beyond leading power*, *Nucl. Phys.* **B643** (2002) 431–476, [[hep-ph/0206152](#)].
- [67] S. R. Klein, J. Nystrand, J. Seger, Y. Gorbunov and J. Butterworth, *STARlight: A Monte Carlo simulation program for ultra-peripheral collisions of relativistic ions*, *Comput. Phys. Commun.* **212** (2017) 258–268, [[1607.03838](#)].
- [68] M. G. A. Buffing, Z.-B. Kang, K. Lee and X. Liu, *A transverse momentum dependent framework for back-to-back photon+jet production*, [1812.07549](#).
- [69] R. F. del Castillo, M. G. Echevarria, Y. Makris and I. Scimemi, *TMD factorization for di-jet and heavy meson pair in DIS*, [2008.07531](#).

- [70] R. F. del Castillo, M. G. Echevarria, Y. Makris and I. Scimemi, *Transverse momentum dependent distributions in dijet and heavy hadron pair production at EIC*, *JHEP* **03** (2022) 047, [[2111.03703](#)].
- [71] M. Cacciari, G. P. Salam and G. Soyez, *The anti- k_t jet clustering algorithm*, *JHEP* **04** (2008) 063, [[0802.1189](#)].
- [72] T. Becher and M. Neubert, *Drell-Yan Production at Small q_T , Transverse Parton Distributions and the Collinear Anomaly*, *Eur. Phys. J. C* **71** (2011) 1665, [[1007.4005](#)].
- [73] T. Becher, M. Neubert and D. Wilhelm, *Electroweak Gauge-Boson Production at Small q_T : Infrared Safety from the Collinear Anomaly*, *JHEP* **02** (2012) 124, [[1109.6027](#)].
- [74] J.-y. Chiu, A. Jain, D. Neill and I. Z. Rothstein, *The Rapidity Renormalization Group*, *Phys. Rev. Lett.* **108** (2012) 151601, [[1104.0881](#)].
- [75] J.-Y. Chiu, A. Jain, D. Neill and I. Z. Rothstein, *A Formalism for the Systematic Treatment of Rapidity Logarithms in Quantum Field Theory*, *JHEP* **05** (2012) 084, [[1202.0814](#)].
- [76] Z.-B. Kang, K. Lee, D. Y. Shao and J. Terry, *The Sivers Asymmetry in Hadronic Dijet Production*, *JHEP* **02** (2021) 066, [[2008.05470](#)].
- [77] F. Caola, A. Von Manteuffel and L. Tancredi, *Diphoton Amplitudes in Three-Loop Quantum Chromodynamics*, *Phys. Rev. Lett.* **126** (2021) 112004, [[2011.13946](#)].
- [78] S. D. Ellis, C. K. Vermilion, J. R. Walsh, A. Hornig and C. Lee, *Jet Shapes and Jet Algorithms in SCET*, *JHEP* **11** (2010) 101, [[1001.0014](#)].
- [79] G. Bell, R. Rahn and J. Talbert, *Generic dijet soft functions at two-loop order: correlated emissions*, *JHEP* **07** (2019) 101, [[1812.08690](#)].
- [80] J. C. Collins, D. E. Soper and G. F. Sterman, *Transverse Momentum Distribution in Drell-Yan Pair and W and Z Boson Production*, *Nucl. Phys. B* **250** (1985) 199–224.
- [81] A. Bacchetta, F. Delcarro, C. Pisano, M. Radici and A. Signori, *Extraction of partonic transverse momentum distributions from semi-inclusive deep-inelastic scattering, Drell-Yan and Z-boson production*, *JHEP* **06** (2017) 081, [[1703.10157](#)].
- [82] H.-S. Shao and D. d’Enterria, *gamma-UPC: Automated generation of exclusive photon-photon processes in ultraperipheral proton and nuclear collisions with varying form factors*, [2207.03012](#).